Desalination and Water Treatment
www.deswater.com

doi: 10.5004/dwt.2017.21308

85 (2017) 313–319
August

Rapid removal of aqueous Cr(VI) and the removal mechanism using ZVI/Fe_3O_4/Fe^{2+} system

Long Zhang, Fenglian Fu*, Zecong Ding, Jiabin Pang

School of Environmental Science and Engineering, Guangdong University of Technology, Guangzhou 510006, China, email: fufenglian2006@163.com (F. Fu)

Received 31 March 2017; Accepted 4 August 2017

ABSTRACT

The treatment of chromium wastewater is a global environmental issue. In this paper, the influencing factors such as initial pH and Fe^{2+} concentration on the removal of Cr(VI) by the zero-valent iron (ZVI)/Fe_3O_4/Fe^{2+} system were studied. The comparison of Cr(VI) removal by hybrid ZVI/Fe_3O_4/Fe^{2+} system, non-hybrid, and partial-hybrid systems were studied. Fe(II)/Fe_T and Fe(III)/Fe_T changes, and Cr(III) concentration change were also investigated. X-ray powder diffraction, Fourier transform infrared spectroscopy, and X-ray photoelectron spectroscopy were used to study the reaction mechanism between Cr(VI) and the ZVI/Fe_3O_4/Fe^{2+} system. The removal of Cr(VI) was accelerated with the increase of Fe^{2+} concentrations and decrease of initial pH. Cr(VI) from synthetic wastewater reduced from initial 20.0 to 0.1 mg/L in 30 min by 2.5 g/L ZVI, 2.5 g/L Fe_3O_4, and 0.4 mM Fe^{2+} at initial pH 3.0. At initial pH value of 3.0, Fe(II) and Fe(III) generation–consumption–regeneration cycle in the ZVI/Fe_3O_4/Fe^{2+} system was studied. The characterization of the ZVI/Fe_3O_4 after the reaction revealed that the removal of Cr(VI) is a complex process including surface adsorption and reduction. This study demonstrates that the ZVI/Fe_3O_4/Fe^{2+} system has a great potential to be applied in treating wastewater containing Cr(VI).

Keywords: ZVI/Fe_3O_4/Fe^{2+}; Cr(VI); Removal mechanism

1. Introduction

The treatment of chromium wastewater is a global environmental issue. Chromium is necessary to the mankind health [1]. Chromium compounds are necessary to many industries including wood preservation, electroplating, steel production, nuclear power plant, leather tanning, anodizing of aluminum, chromate preparation, water cooling, and textile industries [2]. In solution, chromium is found in two stable oxidation states including Cr(VI) and Cr(III) [3]. The Cr(VI) is 500 times more poisonous than the Cr(III), and Cr(VI) is a potent carcinogenic and mutagenic element [2,4]. The emissions of Cr(VI) to the earth's surface water are controlled to under 0.05 mg/L by the US EPA, but total Cr (including Cr(VI) and Cr(III)) is controlled to under 2.0 mg/L [5].

Some technologies have been used in the removal of Cr(VI) from solution, such as adsorption [6,7], electrochemical reduction [8,9], electrocoagulation [10,11], ion exchange [12,13], and membrane separation [14,15]. But the above traditional Cr(VI) treatment methods present both economic and technological challenges [16]. Therefore, it is very significant to explore a more inexpensive, effective, and simple method to remove Cr(VI).

Among the various treatment technologies of Cr(VI), zero-valent metal based technology is a promising approach. The most widely used zero-valent metal is zero-valent iron (ZVI). More and more attention has been paid to the ZVI in treating contaminants in wastewater, because it has the characteristics of simple composition, simple technological process with fine adaptability, and low cost [17]. ZVI can effectively remove selenate [16,18], organic compound [19,20], nitrate [21,22], and heavy metal [23,24]. The mechanism of removing pollutants using ZVI is mainly through

---

* Corresponding author.

1944-3994/1944-3986

the reduction, microelectrolysis, and adsorption [25]. But ZVI has several limitations, including surface passivation, low reactivity, and quick deactivation. Because the Fe_3O_4 and Fe^{2+} can sustain ZVI system's reactivity for contaminants reduction and overcome ZVI surface passivation, it is supposed that the hybridized ZVI/Fe_3O_4/Fe^{2+} system could more effectively remove contaminants. According to the report from Tang et al. [16], the removal of selenate by ZVI/Fe_3O_4/Fe^{2+} system possessed a better performance.

In this study, the removal of Cr(VI) by ZVI/Fe_3O_4/Fe^{2+} system was investigated. The influential factors for Cr(VI) removal including initial pH and Fe^{2+} concentration in ZVI/Fe_3O_4/Fe^{2+} system was studied. The performance of the hybrid ZVI/Fe_3O_4/Fe^{2+} system was compared with those of non-hybrid or partial-hybrid systems. At different initial pH values, Cr(III) concentration change, Fe(II)/Fe_{total} (Fe_T), and Fe(III)/Fe_T changes were investigated. X-ray powder diffraction (XRD), Fourier transform infrared spectroscopy (FT-IR), and X-ray photoelectron spectroscopy (XPS) were employed to characterize the ZVI/Fe_3O_4 before and after the reaction with Cr(VI), so as to indicate the properties, composition, and structure of ZVI/Fe_3O_4 as well as the Cr(VI) removal mechanism.

2. Materials and methods

2.1. Materials

All chemicals were of analytical grade and were used without further purification. All solutions were prepared with deionized water. Fe_3O_4 (Fe_3O_4, powder, >99.9%) was purchased from Damao Chemicals, China. ZVI (Fe, powder, >98.0%) was purchased from Kelong Chemicals, China. Stock solutions of Cr(VI) and Fe^{2+} were prepared by dissolving $K_2Cr_2O_7$ ($K_2Cr_2O_7$, crystal, >99.8%) and $FeCl_2$ ($FeCl_2 \cdot 4H_2O$, crystal, >99.5%) to a final concentration of 500.0 mg/L Cr(VI) and 0.1 M Fe^{2+}, respectively. Solutions of Cr(VI) used during the experiment were prepared by diluting the stock solution to 20.0 mg/L.

2.2. Batch experiments

A certain amount of ZVI and Fe_3O_4 powder and the $FeCl_2$ solution was added into 200.0 mL of 20.0 mg/L Cr(VI) solutions. The solution was regularly sampled and immediately filtered. Then, the residual Cr(VI) and Fe(II) concentrations in the filtrate were determined. To study the effect of pH values on the Cr(VI) removal, initial pH values of the solutions were regulated to 3.0, 5.0, 7.0, and 9.0 at ambient temperature by using 0.1 M HCl or NaOH solutions. The pH value was measured using a pH meter (PHS-3C, Shanghai, China).

2.3. Analytical methods

The amount of Cr(VI) in solution was determined with 1,5-diphenylcarbazide colorimetric method using a UV-2400 spectrophotometer (Shanghai, China) (λ_{max} = 540 nm). The residual Fe(II) concentration in the filtrate was determined with the 1,10-phenanthroline colorimetric method at 510 nm, using a UV-2400 spectrophotometer. Residual total chromium and total iron concentrations in solution were measured using a flame atomic absorption spectrometer (AAS, Z-2000, Hitachi, Japan). The difference between total chromium and Cr(VI) was calculated as the concentration of Cr(III). In the same way, Fe(III) concentration can be obtained.

2.4. Characterization methods

The XRD spectra of the ZVI/Fe_3O_4 before and after reaction were obtained from an X-ray powder diffractometer (Rigaku, Japan) at 36.0 kV and 20.0 mA with Cu Kα radiation.

The FT-IR spectra of the ZVI/Fe_3O_4 before and after reaction were recorded on a Nicolet 6700 (Thermo Fisher Scientific, USA) spectrometer at the wavenumber range of 4,000–400 cm^{-1}.

The XPS spectra of ZVI/Fe_3O_4 before and after reaction were conducted with an Amicus (Shimadzu Co., Japan) X-ray photoelectron spectrometer with monochromatic Al Kα radiation. The curve fitting used mixed Gaussian–Lorentzian functions, and the spectra before and after the ZVI/Fe_3O_4 were deconvoluted into peaks with the software XPSPEAK from RCSMS lab.

3. Results and discussion

3.1. Characterization

3.1.1. XRD analysis of the ZVI/Fe_3O_4/Fe^{2+} system

The XRD spectra of ZVI/Fe_3O_4 before reaction are shown in Fig. 1(a). The XRD pattern of ZVI revealed the diffraction peaks at 44.7° and 65.0°, and the diffraction peaks of Fe_3O_4 can be detected at 30.3°, 35.6°, 43.1°, 57.2°, and 62.7°.

Meanwhile, there were some new diffraction peaks in XRD spectra of ZVI/Fe_3O_4 after reaction (Fig. 1(b)), such as $FeCr_2O_4$ (the diffraction peaks at 30.1°, 35.5°, 43.1°, 57.1°, and 62.7°), which indicated that new compounds generated on the surface of the ZVI/Fe_3O_4. But the intensity of ZVI/Fe_3O_4 peaks decreased after reaction. According to the report by Yeh et al. [26], the decreased intensity of ZVI/Fe_3O_4 peaks after reaction was likely attributed to the lattice strain caused by the differences of various atomic sizes.

3.1.2. FT-IR analysis of the ZVI/Fe_3O_4/Fe^{2+} system

The FT-IR spectra of the original ZVI/Fe_3O_4 are shown in Fig. 2(a). The band at 436.4 and 562.4 cm^{-1} was assigned to the Fe–O [27]. The band at 1,631.6 cm^{-1} was assigned to the bending vibration of water [27].

The FT-IR spectra of the ZVI/Fe_3O_4 after reaction with Cr(VI) are shown in Fig. 2(b). After the reaction, the band at 3,442.0 and 1,631.6 cm^{-1} was assigned to stretching of the O–H and the bending vibration of water [27], respectively. The absorption bands at 436.4 cm^{-1} shifted to 446.5 cm^{-1} after reaction. Furthermore, the bands at 585.9 and 632.0 cm^{-1} were assigned to the formation of Fe–O–Cr on ZVI/Fe_3O_4 surface [28,29], which was confirmed in the results of the XPS. All these observations indicated that Fe–Cr hydroxide precipitates probably formed on the surface of ZVI/Fe_3O_4 after reaction.

3.2. Cr(VI) removal by the ZVI/Fe_3O_4/Fe^{2+} system

3.2.1. Cr(VI) removal in different systems

Removal of Cr(VI) in different systems is illustrated in Fig. 3. It can be seen that residual Cr(VI) concentration varied

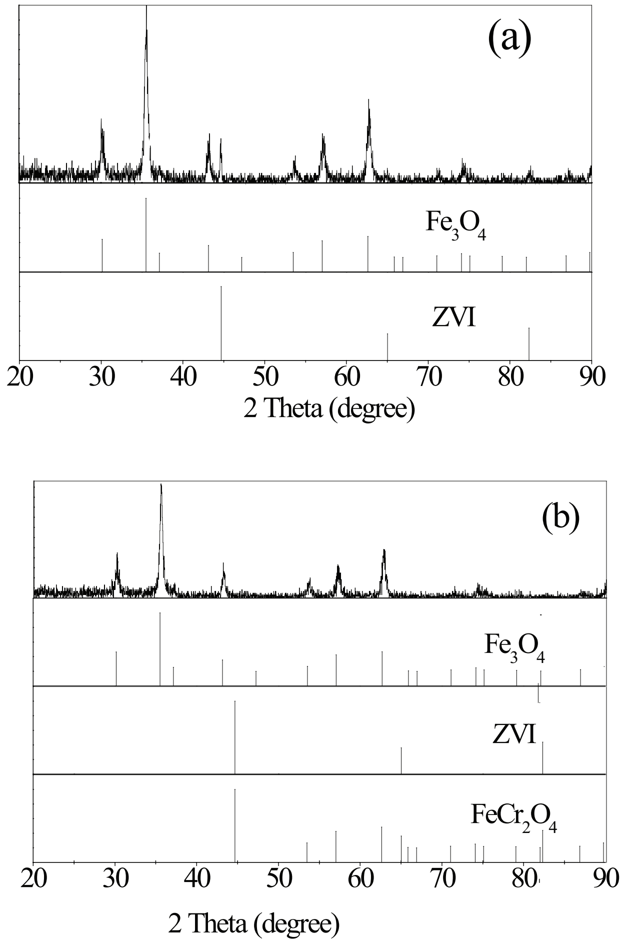

Fig. 1. XRD of ZVI/Fe_3O_4 (a) before reaction and (b) after reaction.

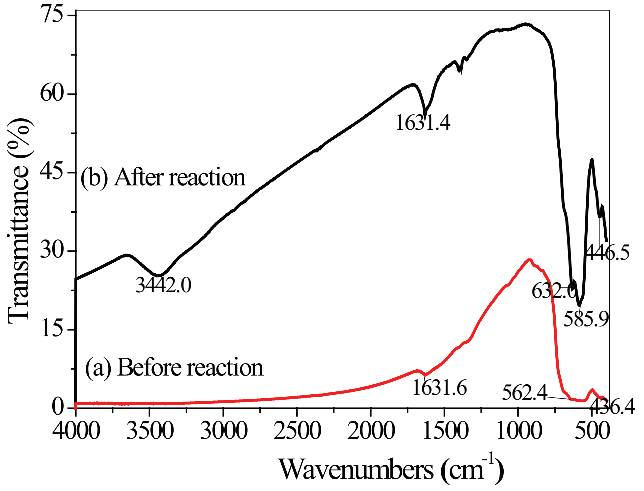

Fig. 2. FT-IR spectra for ZVI/Fe_3O_4 (a) before reaction and (b) after reaction.

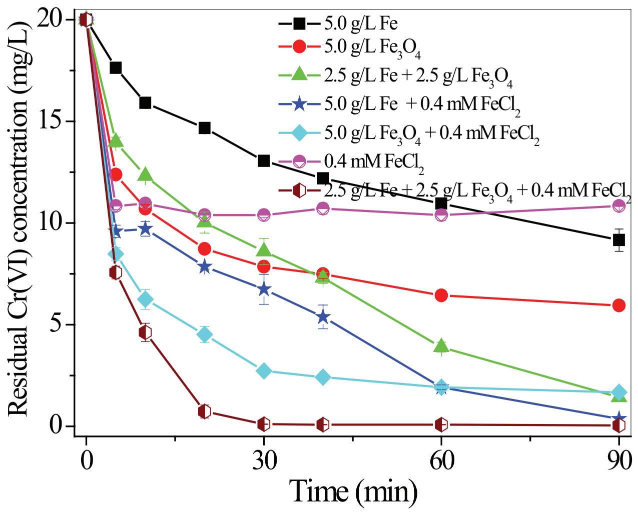

Fig. 3. Cr(VI) removal in different systems ($[Cr(VI)]_0 = 20.0$ mg/L, $[ZVI]_0 = 2.5$ g/L, $[Fe_3O_4]_0 = 2.5$ g/L, $[Fe^{2+}]_0 = 0.4$ mM, $pH_0 = 3.0$).

in different systems. In the ZVI system, about 13.1 mg/L Cr(VI) still remained after 30 min. This is because Cr(VI) is deoxidated to Cr(III) by ZVI (Eq. (1)). The generated Cr^{3+} and Fe^{3+} can form $Cr_xFe_{1-x}(OH)_3$ precipitates (Eq. (2)). The hydroxide precipitates covered the ZVI surface, so the reactions slowed over time. In the Fe^{2+} system, Cr(VI) concentration decreased from initial 20.0 mg/L quickly to 10.8 mg/L in the first 5 min, and remained nearly unchanged after 5 min. It might be because Fe^{2+} was nearly consumed in the first 5 min because the reaction of Cr(VI) with Fe^{2+} was very fast (Eq. (3)). In Fe_3O_4 system, Cr(VI) concentration decreased from initial 20.0 to 7.9 mg/L after 30 min. All above results suggested that single ZVI, Fe^{2+}, and Fe_3O_4 cannot efficiently remove Cr(VI) from wastewater.

$$Fe + CrO_4^{2-} + 8H^+ \rightarrow Fe^{3+} + Cr^{3+} + 4H_2O \tag{1}$$

$$xCr^{3+} + (1-x)Fe^{3+} + 3H_2O \rightarrow Cr_xFe_{1-x}(OH)_3\,(s) + 3H^+ \tag{2}$$

$$3Fe^{2+} + CrO_4^{2-} + 8H^+ \rightarrow 3Fe^{3+} + Cr^{3+} + 4H_2O \tag{3}$$

In the ZVI/Fe^{2+}, Fe_3O_4/Fe^{2+}, and ZVI/Fe_3O_4 systems, Cr(VI) concentrations reduced from initial 20.0 mg/L to 6.7, 2.7, and 8.6 mg/L after 30 min, respectively. The data suggested that two components combined systems among the ZVI, Fe_3O_4, and Fe^{2+} cannot effectively remove Cr(VI).

The ZVI/Fe_3O_4/Fe^{2+} system exhibited the highest Cr(VI) removal efficiency, Cr(VI) concentration was reduced from initial 20.0 to 0.1 mg/L within 30 min. The highest Cr(VI) removal efficiency by the ZVI/Fe_3O_4/Fe^{2+} system may be because the ZVI/Fe_3O_4/Fe^{2+} system comprised several sub-systems, such as ZVI, Fe_3O_4, Fe^{2+}, ZVI/Fe^{2+}, Fe_3O_4/Fe^{2+}, and ZVI/Fe_3O_4 systems, all the sub-systems contribute to removal of Cr(VI) in the ZVI/Fe_3O_4/Fe^{2+} system. Another reason could be that the synergetic effect and the reciprocity among the ZVI, Fe_3O_4, and Fe^{2+} promoted to rapid removal of Cr(VI). The possible pathways for Cr(VI) removal in ZVI/Fe_3O_4/Fe^{2+} system were: (1) Cr(VI) adsorption onto the ZVI/Fe_3O_4 surface, and (2) Cr(VI) direct reduction on the ZVI/Fe_3O_4 surface by ZVI and Fe^{2+} (Eqs. (1) and (3)).

3.2.2. Effect of Fe^{2+} concentration on Cr(VI) removal

Effect of Fe^{2+} concentration on Cr(VI) removal in the ZVI/Fe_3O_4/Fe^{2+} system is illustrated in Fig. 4. In the ZVI/Fe_3O_4

system (without Fe^{2+} addition), Cr(VI) residual concentration was 8.6 mg/L after 30 min. In the presence of 0.1, 0.2, 0.3, 0.4, and 0.5 mM Fe^{2+}, Cr(VI) removal obviously accelerated and Cr(VI) concentration decreased from initial 20.0 mg/L quickly to 4.9, 6.2, 2.3, 0.1, and 0.1 mg/L in the first 30 min, respectively. All above results demonstrated that the important effect of Fe^{2+} dramatically accelerated the removal of Cr(VI) in ZVI/Fe_3O_4/Fe^{2+} system and the Cr(VI) removal increased with the increasing Fe^{2+} concentration.

In addition, from section 3.2.1, 0.4 mM Fe^{2+} can remove 9.2 mg/L Cr(VI) in solution. From Eq. (4), ZVI reaction with Fe^{3+} can generate Fe^{2+}. Based on the above points, it can be inferred that the Fe^{2+} not only directly participated in the Cr(VI) reduction but also could rejuvenate in the surface of ZVI by Fe(II) and Fe(III) generation–consumption–regeneration cycle, favoring electron transfer for Cr(VI) reduction.

$$Fe + 2Fe^{3+} = 3Fe^{2+} \tag{4}$$

3.2.3. Effect of initial pH on Cr(VI) removal

Removal of Cr(VI) in different initial pH values is illustrated in Fig. 5. At initial pH value of 3.0, 5.0, 7.0, and 9.0, Cr(VI) concentrations reduced from initial 20.0 mg/L to 0.1, 4.6, 4.8, and 4.6 mg/L after 30 min, respectively. So the Cr(VI) removal efficiencies increased with the decreasing initial pH values. In acidic condition, the corrosion of ZVI generated Fe^{2+} and the release of Fe^{2+} increased the Cr(VI) removal (Eq. (5)). In alkaline and neutral conditions, $Fe(OH)_2$ and $Fe(OH)_3$ precipitates formed and covered the surface of the ZVI, and impeded reaction between the ZVI and Cr(VI) (Eqs. (6)–(9)):

$$2Fe^0 + O_2 + 4H^+ \rightarrow 2Fe^{2+} + 2H_2O \tag{5}$$

$$Fe^{2+} + 2H_2O \rightarrow Fe(OH)_2 + 2H^+ \tag{6}$$

$$Fe^{3+} + 3H_2O \rightarrow Fe(OH)_3 + 3H^+ \tag{7}$$

$$Fe^{2+} + 2OH^- \rightarrow Fe(OH)_2 \tag{8}$$

$$Fe^{3+} + 3OH^- \rightarrow Fe(OH)_3 \tag{9}$$

According to the inset in Fig. 5, at initial pH value of 3.0, the reaction of ZVI and Fe^{2+} with Cr(VI) consumed H^+ (Eqs. (1) and (3)), which led to the pH value increase over time. At initial pH value of 5.0, 7.0, and 9.0, the pH value decreased rapidly from initial 5.0, 7.0, and 9.0 to 3.7, 4.2, and 4.6 in the first 1 min, respectively. It could be because the hydrolysis of Fe^{2+} generated H^+ (Eq. (6)).

3.2.4. Cr(III) concentration change at different initial pH

In order to study the Cr(VI) reduction characteristics on the ZVI/Fe_3O_4/Fe^{2+} system, Cr(III) concentration change in different initial pH values is illustrated in Fig. 6. At initial pH of 3.0, 7.0, and 9.0, Cr(III) residual concentrations were 4.2, 1.2, and 0 mg/L after reaction for 90 min. So the Cr(III) residual concentrations decreased with the increase of initial pH values. It might be because surface adsorption of the ZVI/Fe_3O_4 and the formation of Fe–Cr hydroxide/oxyhydroxide and Cr(III) hydroxide precipitates were reduced in acidic condition. In alkaline and neutral conditions, the Fe–Cr hydroxide/oxyhydroxide and Cr(III) hydroxide precipitates formed more easily (Eqs. (2) and (10)):

$$Cr^{3+} + 3OH^- \rightarrow Cr(OH)_3 \tag{10}$$

3.2.5. Fe(II)/Fe_T and Fe(III)/Fe_T changes at different initial pH values

For better understanding the ZVI/Fe_3O_4/Fe^{2+} system with Cr(VI) reaction characteristics, Fe(II)/Fe_T and Fe(III)/Fe_T changes in different initial pH values are illustrated in Fig. 7. At initial pH value of 3.0 (Fig. 7(a)), Fe(II) and Fe(III)

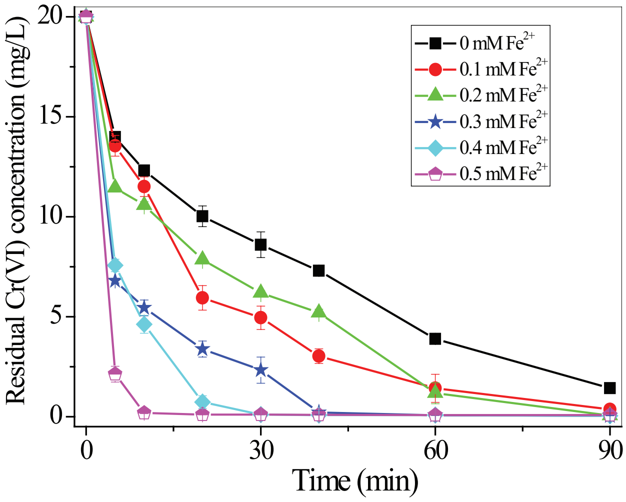

Fig. 4. Effect of Fe^{2+} concentration on Cr(VI) removal in the ZVI/Fe_3O_4/Fe^{2+} system ($[Cr(VI)]_0$ = 20.0 mg/L, $[ZVI]_0$ = 2.5 g/L, $[Fe_3O_4]_0$ = 2.5 g/L, pH_0 = 3.0).

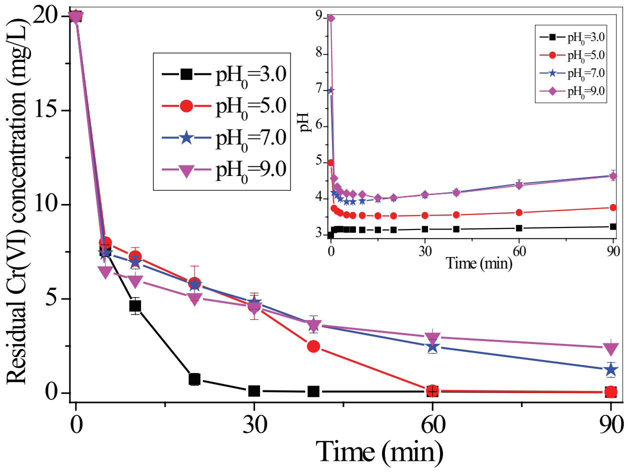

Fig. 5. Effect of initial pH on the Cr(VI) removal ($[Cr(VI)]_0$ = 20.0 mg/L, $[ZVI]_0$ = 2.5 g/L, $[Fe_3O_4]_0$ = 2.5 g/L, $[Fe^{2+}]_0$ = 0.4 mM). Inset: pH changes in the reaction process.

generation–consumption–regeneration cycle in the ZVI/Fe_3O_4/Fe^{2+} system was found. This was consistent with the result obtained in section 3.2.2. Fe(II)/Fe_T rapidly decreased and accordingly Fe(III)/Fe_T rapidly increased during the first 10 min. This phenomenon was attributed to the fact that Fe^{2+} was consumed due to Fe^{2+} reaction with Cr(VI) (Eq. (3)). Furthermore, Fe(II)/Fe_T increased and Fe(III)/Fe_T decreased from 10 to 90 min. It may be because the residual ZVI generated Fe^{2+} (Eq. (5)) and ZVI reaction with Fe^{3+} generated Fe^{2+} (Eq. (4)).

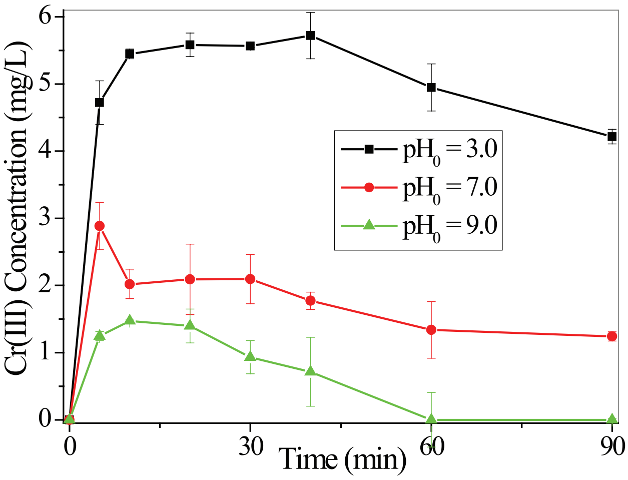

Fig. 6. Effect of varied initial pH values on Cr(III) concentration changes ($[Cr(VI)]_0 = 20.0$ mg/L, $[ZVI]_0 = 2.5$ g/L, $[Fe_3O_4]_0 = 2.5$ g/L, $[Fe^{2+}]_0 = 0.4$ mM).

As can be seen in Figs. 7(b) and (c), at initial pH of 7.0 and 9.0, Fe(II)/Fe_T decreased quickly to 0 and Fe(III)/Fe_T rapidly increased to 1.0 with the reaction proceeding in the first 5 min, but the Fe(II)/Fe_T and Fe(III)/Fe_T remained nearly unchanged after 5 min. This might be because Fe^{2+} and Fe^{3+} are easy to form $Fe(OH)_2$ and $Fe(OH)_3$ (or FeOOH) precipitates in alkaline and neutral conditions (Eqs. (6)–(9)).

3.3. XPS analysis of the ZVI/Fe_3O_4/Fe^{2+} system

In order to further validate the chemical oxidation states and elemental composition of the samples, XPS analysis for ZVI/Fe_3O_4/Fe^{2+} system was carried out. All spectra were calibrated using C 1s (284.6 eV) as the reference.

As shown in Fig. 8(a), XPS analysis revealed that Fe, C, and O were present on the surface of ZVI/Fe_3O_4. Before reaction, the ZVI/Fe_3O_4 surface was dominated by Fe (24.23%), O (48.97%), and C (26.8%). After reaction, ZVI surface composition was Fe (21.17%), O (50.21%), Cr (0.02%), and C (26.09%).

Fig. 8(b) presents the XPS Fe 2p spectrum of ZVI/Fe_3O_4 after reaction. The broad peak of Fe $2p_{3/2}$ could be fitted to three peaks at the binding energies of 709.2, 710.2, and 711.2 eV, which are the characteristics of Fe(II), Fe(III), and Fe(III) in Fe_3O_4 [30], respectively. The Fe $2p_{1/2}$ peaks centered at binding energies of 724.1 eV, which represented

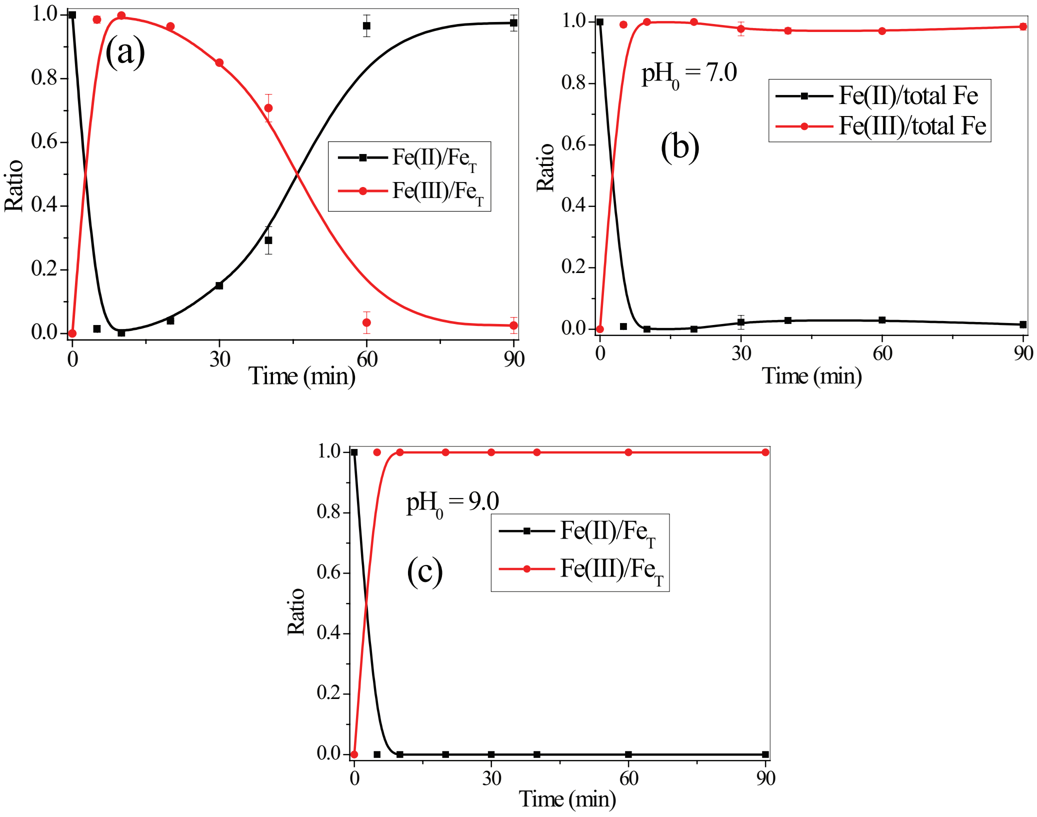

Fig. 7. Fe(II)/Fe_T and Fe(III)/Fe_T changes at different initial pH values ($[Cr(VI)]_0 = 20.0$ mg/L, $[ZVI]_0 = 2.5$ g/L, $[Fe_3O_4]_0 = 2.5$ g/L, $[Fe^{2+}]_0 = 0.4$ mM) ((a) $pH_0 = 3.0$, (b) $pH_0 = 7.0$, and (c) $pH_0 = 9.0$).

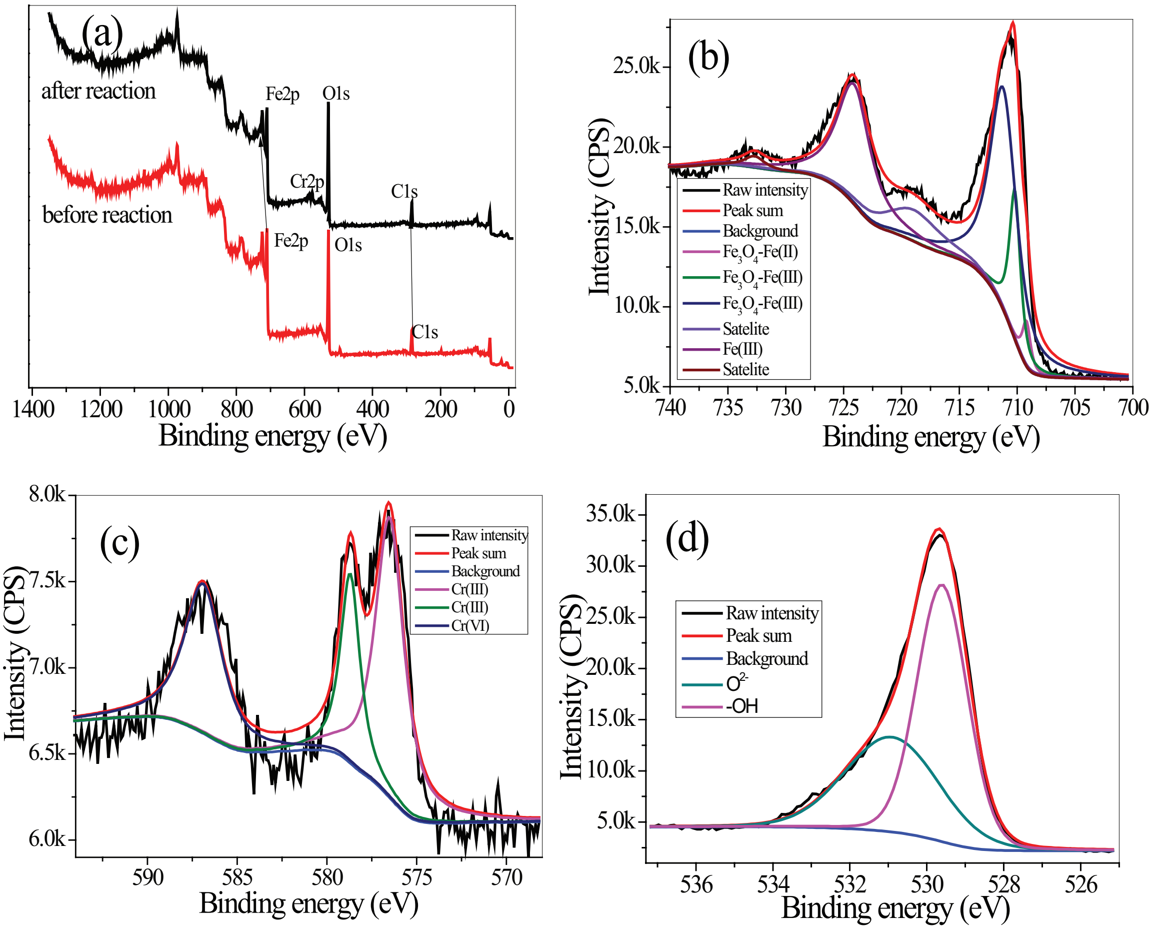

Fig. 8. XPS survey (a) before reaction, and after reaction of (b) Fe, (c) Cr, and (d) O.

Fe(III) [31]. In addition, the satellite peak at 718.9 eV was the satellite peak of Fe $2p_{3/2}$. Another satellite peak at 732.7 eV was the satellite peak of Fe $2p_{1/2}$.

After Cr(VI) removal, the Cr 2p spectra from ZVI/Fe_3O_4 was investigated (Fig. 8(c)). Results show that the Cr $2p_{1/2}$ peak centered at 587.2 eV, and the data matches well with Cr(VI) [32], so removal process of Cr(VI) included surface adsorption. The broad peak of Cr $2p_{3/2}$ could be fitted to two peaks at binding energies of 576.5 and 578.6 eV, which are the characteristics of Cr(III) species [30], so removal process of Cr(VI) included reduction. Furthermore, the peaks between 575 and 580 eV indicated that Fe(III)–Cr(III) hydroxide/oxyhydroxide formed in the reaction [30].

In XPS spectra of O 1s (Fig. 8(d)), the binding energies at 529.6 and 530.9 eV represented O^{2-} and OH^- [33], respectively. OH^- occupied 40.7% of the O, while O^{2-} occupied 59.3%, which indicated that hydroxides formed on the surface of ZVI/Fe_3O_4.

In a word, Cr(VI) was reduced to Cr(III), which was subsequently formed Cr(III) hydroxide precipitates [34]. Due to the same charge and closer ionic radii between Fe(III) and Cr(III), they can easily form a mixed Fe(III)–Cr(III) hydroxide/oxyhydroxide [35]. Therefore, Cr(VI) was removed through the formation of Fe(III)–Cr(III) hydroxide/oxyhydroxide and Cr(III) hydroxide on the surface of the ZVI/Fe_3O_4.

4. Conclusions

In this study, the ZVI/Fe_3O_4/Fe^{2+} system was employed to treat Cr(VI) wastewater. Results demonstrated that the ZVI/Fe_3O_4/Fe^{2+} system exhibited a great capacity to remove Cr(VI) than those of non-hybrid or partial-hybrid systems. Cr(VI) removal by ZVI/Fe_3O_4/Fe^{2+} system was effected by initial pH and Fe^{2+} concentration. Cr(VI) removal increased with the increase of Fe^{2+} concentrations and decrease of pH values. At initial pH value of 3.0, in the ZVI/Fe_3O_4/Fe^{2+} system, Fe^{2+} not only directly participated in the Cr(VI) reduction but also could rejuvenate in the surface of ZVI, by Fe(II) and Fe(III) generation–consumption–regeneration cycle favoring electron transfer for Cr(VI) reduction. Cr(III) residual concentrations decreased with the increase of initial pH values. The characterization of the ZVI/Fe_3O_4 demonstrated that the removal of Cr(VI) was a complicated process including surface adsorption and reduction. The ZVI/Fe_3O_4/Fe^{2+} has a great potential to be applied in treating wastewater containing Cr(VI).

Acknowledgments

This research was supported by the National Natural Science Foundation of China (No. 51008084), Science and Technology Planning Project of Guangdong Province (No. 2016A020221032), and Development Program for

Outstanding Young Teachers in Guangdong Province (No. Yq2013055).

References

[1] J. Lyu, L. Zhu, C. Burda, Optimizing nanoscale TiO_2 for adsorption-enhanced photocatalytic degradation of low-concentration air pollutants, ChemCatChem, 5 (2013) 3114–3123.

[2] S. Yadav, V. Srivastava, S. Banerjee, C.H. Weng, Y.C. Sharma, Adsorption characteristics of modified sand for the removal of hexavalent chromium ions from aqueous solutions: kinetic, thermodynamic and equilibrium studies, Catena, 100 (2013) 120–127.

[3] M. Bhaumik, A. Maity, V.V. Srinivasu, M.S. Onyango, Removal of hexavalent chromium from aqueous solution using polypyrrole-polyaniline nanofibers, Chem. Eng. J., 18 (2012) 323–333.

[4] E. Petala, M. Baikousi, M.A. Karakassides, G. Zoppellaro, J. Filip, J. Tuček, K.C. Vasilopoulos, J. Pechoušek, R. Zbořil, Synthesis, physical properties and application of the zero-valent iron/titanium dioxide heterocomposite having high activity for the sustainable photocatalytic removal of hexavalent chromium in water, Phys. Chem. Chem. Phys., 18 (2016) 10637–10646.

[5] V.K. Gupta, A. Rastogi, A. Nayak, Adsorption studies on the removal of hexavalent chromium from aqueous solution using a low cost fertilizer industry waste material, J. Colloid Interface Sci., 342 (2010) 135–141.

[6] R. Karthik, S. Meenakshi, Adsorption study on removal of Cr(VI) ions by polyaniline composite, Desal. Wat. Treat., 54 (2015) 3083–3093.

[7] R. Saha, B. Saha, Removal of hexavalent chromium from contaminated water by adsorption using mango leaves (*Mangifera indica*), Desal. Wat. Treat., 52 (2014) 1928–1936.

[8] Y. Liu, D. Yuan, J. Yan, Q. Li, T. Ouyang, Electrochemical removal of chromium from aqueous solutions using electrodes of stainless steel nets coated with single wall carbon nanotubes, J. Hazard. Mater., 186 (2011) 473–480.

[9] A.S. Dharnaik, P.K. Ghosh, Hexavalent chromium [Cr(VI)] removal by the electrochemical ion-exchange process, Environ. Technol., 35 (2014) 2272–2279.

[10] S. Sadeghi, M.R. Alavi Moghaddam, M. Arami, Improvement of electrocoagulation process on hexavalent chromium removal with the use of polyaluminum chloride as coagulant, Desal. Wat. Treat., 52 (2014) 4818–4829.

[11] F. Akbal, S. Camcı, Copper, chromium and nickel removal from metal plating wastewater by electrocoagulation, Desalination, 269 (2011) 214–222.

[12] L. Alvarado, I.R. Torres, A. Chen, Integration of ion exchange and electrodeionization as a new approach for the continuous treatment of hexavalent chromium wastewater, Sep. Purif. Technol., 105 (2013) 55–62.

[13] R. Gayathri, P.S. Kumar, Recovery and reuse of hexavalent chromium from aqueous solutions by a hybrid technique of electrodialysis and ion exchange, Braz. J. Chem. Eng., 27 (2010) 71–78.

[14] G. Basaran, D. Kavak, N. Dizge, Y. Asci, M. Solener, B. Ozbey, Comparative study of the removal of nickel (II) and chromium (VI) heavy metals from metal plating wastewater by two nanofiltration membranes, Desal. Wat. Treat., 57 (2016) 21870–21880.

[15] S. Habibi, A. Nematollahzadeh, S.A. Mousavi, Nano-scale modification of polysulfone membrane matrix and the surface for the separation of chromium ions from water, Chem. Eng. J., 267 (2015) 306–316.

[16] C. Tang, Y. Huang, Z. Zhang, J. Chen, H. Zeng, Y.H. Huang, Rapid removal of selenate in a zero-valent iron/Fe_3O_4/Fe^{2+} synergetic system, Appl. Catal., B, 184 (2016) 320–327.

[17] R. Singh, V. Misra, R.P. Singh, Synthesis, characterization and role of zero-valent iron nanoparticle in removal of hexavalent chromium from chromium-spiked soil, J. Nanopart. Res., 13 (2011) 4063–4073.

[18] I.H. Yoon, S. Bang, K.W. Kim, M.G. Kim, S.Y. Park, W.K. Choi, Selenate removal by zero-valent iron in oxic condition: the role of Fe(II) and selenate removal mechanism, Environ. Sci. Pollut. Res., 23 (2016) 1081–1090.

[19] X. Wang, L. Wang, J. Li, J. Qiu, C. Cai, H. Zhang, Degradation of acid orange 7 by persulfate activated with zero valent iron in the presence of ultrasonic irradiation, Sep. Purif. Technol., 122 (2014) 41–46.

[20] H. Chen, Y. Cao, E. Wei, T. Gong, Q. Xian, Facile synthesis of graphene nano zero-valent iron composites and their efficient removal of trichloronitromethane from drinking water, Chemosphere, 146 (2016) 32–39.

[21] Y. Lubphoo, J.M. Chyan, N. Grisdanurak, C.H. Liao, Influence of Pd–Cu on nanoscale zero–valent iron supported for selective reduction of nitrate, J. Taiwan Inst. Chem. Eng., 59 (2016) 285–294.

[22] A.M.E. Khalil, O. Eljamal, S. Jribi, N. Matsunaga, Promoting nitrate reduction kinetics by nanoscale zero valent iron in water via copper salt addition, Chem. Eng. J., 287 (2016) 367–380.

[23] X. Guo, Z. Yang, H. Dong, X. Guan, Q. Ren, X. Lv, X. Jin, Simple combination of oxidants with zero-valent-iron (ZVI) achieved very rapid and highly efficient removal of heavy metals from water, Water Res., 88 (2016) 671–680.

[24] M.J. López-Muñoz, A. Arencibia, Y. Segura, J.M. Raez, Removal of As(III) from aqueous solutions through simultaneous photocatalytic oxidation and adsorption by TiO_2 and zero-valent iron, Catal. Today, 280 (2017) 149–154.

[25] A. Shimizu, M. Tokumura, K. Nakajima, Y. Kawase, Phenol removal using zero-valent iron powder in the presence of dissolved oxygen: roles of decomposition by the Fenton reaction and adsorption/precipitation, J. Hazard. Mater., 201 (2012) 60–67.

[26] Y.J.W. Yeh, S.Y. Chang, Y.D. Hong, S.K. Chen, Anomalous decrease in X-ray diffraction intensities of Cu–Ni–Al–Co–Cr–Fe–Si alloy systems with multi-principal elements, Mater. Chem. Phys., 103 (2007) 41–46.

[27] Z. Lu, F. Chen, M. He, M. Song, Z. Ma, W. Shi, Y. Yan, Microwave synthesis of a novel magnetic imprinted TiO_2 photocatalyst with excellent transparency for selective photodegradation of enrofloxacin hydrochloride residues solution, Chem. Eng. J., 249 (2014) 15–26.

[28] F. Luo, Z. Chen, M. Megharaj, R. Naidu, Simultaneous removal of trichloroethylene and hexavalent chromium by green synthesized agarose-Fe nanoparticles hydrogel, Chem. Eng. J., 294 (2016) 290–297.

[29] S. Rajput, C.U. Pittman, D. Mohan, Magnetic magnetite (Fe_3O_4) nanoparticle synthesis and applications for lead (Pb^{2+}) and chromium (Cr^{6+}) removal from water, J. Colloid Interface Sci., 468 (2016) 334–346.

[30] S.R. Chowdhury, E.K. Yanful, A.R. Pratt, Chemical states in XPS and Raman analysis during removal of Cr(VI) from contaminated water by mixed maghemite–magnetite nanoparticles, J. Hazard. Mater., 235 (2012) 246–256.

[31] Y. Mu, H. Wu, Z. Ai, Negative impact of oxygen molecular activation on Cr(VI) removal with core–shell Fe@Fe_2O_3 nanowires, J. Hazard. Mater., 298 (2015) 1–10.

[32] J. Hu, I.M.C. Lo, G. Chen, Performance and mechanism of chromate(VI) adsorption by δ-FeOOH-coated maghemite (γ-Fe_2O_3) nanoparticles, Sep. Purif. Technol., 58 (2007) 76–82.

[33] L. Hao, T. Ouyang, L. Lai, Y.X. Liu, S. Chen, H. Hu, C.T. Chang, J.J. Wang, Temperature effects on arsenate adsorption onto goethite and its preliminary application to arsenate removal from simulative geothermal water, RSC Adv., 4 (2014) 51984–51990.

[34] B. Geng, Z. Jin, T. Li, X. Qi, Preparation of chitosan-stabilized Fe^0 nanoparticles for removal of hexavalent chromium in water, Sci. Total Environ., 407 (2009) 4994–5000.

[35] Y. Zhang, Y. Li, J. Li, G. Sheng, Y. Zhang, X. Zheng, Enhanced Cr(VI) removal by using the mixture of pillared bentonite and zero-valent iron, Chem. Eng. J., 185 (2012) 243–249.